Design and Control of a 3-DOF Rehabilitation Robot for Forearm and Wrist

Lincong Luo, Liang Peng, Zengguang Hou, Weiqun Wang

***Abstract*—This paper presents a 3-DOF compact rehabilitation robot, involving mechanical structure design, control system design and gravity compensation analysis. The robot can simultaneously provide assistance for pronation/supination(P/S), flexion/extension(F/E) and adduction/abduction(A/A) joints rehabilitation training. The P/S and F/E joints are designed to be driven by cable transmission to gain a high backdrivability, and an adjustment plate is adopted to decrease the distance between the rotation axis of F/E joint of the human wrist and the robot. In addition, gravity compensation is considered to offset the impact of self-gravity on the performance of the controller. A "moving window" control strategy based on impedance control is proposed and implemented on the robot. A comparison between the "moving window" control and classical impedance control indicates that the former has more potential to stimulate the voluntary efforts of the participant, and has a less limitation moving in a fixed reference trajectory. Meanwhile, the results also validate the feasibility and safety of the wrist robot system.**

I. Introduction

Stroke is one of the most common causes of hemiplegia and paraplegia, and has a serious impact on the ability of patients to perform activities of daily living (ADL). The intensive rehabilitation therapy is beneficial for patients to regain all or partial motor functions. However, the continuous increase in the number of stroke patients leads to a significant burden for therapists, and thus the intensive rehabilitation training for patients is limited.

Compared to the traditional manual therapy, the robot-assist therapy has the advantage of providing intensive and precision rehabilitation training consistently [1]. Moreover, the measurements recorded by the robotic system during the rehabilitation therapy can be used to assess objectively the performance of patients and help therapists to adjust rehabilitation schemes. In addition, combined with the virtual reality technology, the robot-assist therapy can stimulate voluntary participation of the patients [2]. Many robotic systems have been developed for upper limb rehabilitation, including MIT-Manus [3], T-WREX [4], MIME [5] and ARMin [6]. These systems mainly focus motor therapies on the proximal joints (shoulders and elbows). Several studies about the clinical effectiveness of the rehabilitation robot suggest that the robotic therapies result in improving the strength and motor impairment, but the improvements are not transferred to the ability of performing ADLs [7], [8]. Adding training of the distal arm leads to a further improvement of the motor performance, and can bring benefits to the skill transfer [9], [10].

In this paper, we introduce a 3-DOF compact and backdrivable rehabilitation robot, including the mechanical structure design, control system design and gravity compensation analysis. In addition, a "moving window" control based impedance control is proposed and applied to the robot device. Finally, the feasibility and safety of the wrist rehabilitation robot are validated by primary experiments.

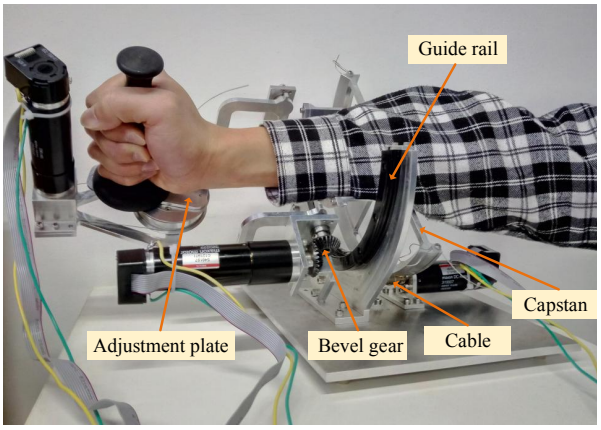

Fig. 1. Mechanical structure of the robot

II. Design and Analysis

A. Mechanism

A human wrist joint in combination with forearm has a 3-DOF motion: pronation/supination (P/S), flexion/extension (F/E), adduction/abduction (A/A). As shown in Fig. 1, we designed a wrist rehabilitation robot device which consists of three revolute joints corresponding to the forearm and the wrist joints, respectively. The robot joints can provide individually assistance for a single wrist joint motion, while the other joints' measurements are not affected.

The electric motors are used to actuate robot joints, because it is easy to design the controller. In addition, the electric motors can meet the requirement of torque, and keep a lower inertia at the same time.

*This research is supported in part by the National Natural Science Foundation of China (Grants 61225017, 61533016, 61421004, 61603386, U1613228), the Strategic Priority Research Program of the CAS (Grant XDB02080000), the Beijing Science and Technology Project (Z161100001516004), and the Early Career Development Award of SKLMCCS.

Lincong Luo is with State Key Laboratory of Management and Control for Complex Systems, Institute of Automation, Chinese Academy of Sciences, Beijing 100190 and University of Chinese Academy of Sciences, Beijing 100049, China{luolincong2014@ia.ac.cn}

Liang Peng, Zengguang Hou and Weiqun Wang are with State Key Laboratory of Management and Control for Complex Systems, Institute of Automation, Chinese Academy of Sciences, Beijing 100190, China{liang.peng@ia.ac.cn, zengguang.hou@ia.ac.cn, weiqun.wang@ia.ac.cn}

The pronation/supination joint is designed using an arc guide rail and slider mechanism. In order to decrease the friction, the P/S and F/E robot joints are driven by the cable transmission rather than the gear transmission. One of the great advantages of the design is the enhancement of backdrivaility of the mechanism. However, to make the mechanical structure compact, the robot's A/A joint is driven by the gear transmission system including a pair of bevel gears.

During rehabilitation training, the subject's forearm is fixed on the cambered forearm-pad, and thus the P/S joint is coaxial with the subject's forearm. Meanwhile, the subject's hand grasps the handle mounted on an adjustment plate, which is used to decrease the distance between the rotation axis of flexion/extension joint of the human wrist and the robot.

The range of motion (ROM) and maximum output torque of each robot's joint are two important characteristics for the wrist rehabilitation training. The former determines the limitation of the wrist motion and the latter is related to assistant capabilities of the robot. The comparison of the ROM and maximum output torque of the robot with the requirements to perform ADLs is shown in Table I.

B. Control Architecture

Each joint of the robot is actuated by a DC brushed motor (Maxon RE30). Each motor is controlled by a servo controller (Maxon ESCON 50/5), which can be configured in current mode or speed mode dependent on the application requirement. To measure the angular position of the robot joint, three encoders with a resolution of 2000 counts per revolution are mounted on the motors. Since the robot has the transmission ratio of 23.6:1, 27.7:1 and 26.9:1 for P/S, A/A and F/E joint, respectively, the minimum measurable angles are 0.0076 degree, 0.0064 degree and 0.0066 degree. Compared to an absolute encoder, these encoders just evaluate the relative position information with respect to the initial position of the joint. Therefore, the encoder values need to be calibrated manually after the robot device is powered on.

The control architecture of the robot is shown in Fig. 2. There are two main tasks implemented in the computer. One is to provide vision feedback for the subject by the virtual environment (video game), where the screen is refreshed according to the measurement of the robot joints in a frequency of 100Hz. The other is to run different rehabilitation training strategies or control loops, such as position tracking, force tracking and impedance control, etc. , where the computer sends expected position or force commands to the microcontroller (ARM STM32103F) and receives the preprocessed state information about the robot from the microcontroller through USB interface in a frequency of 1000Hz .

The microcontroller transforms control commands into Pulse-Width Modulation (PWM) signals or reference voltage signals, which are sent to the motor drive board (ESCON 50/5 module) to actuate the motors. Meanwhile, the information of the sensors is collected and preprocessed by the microcontroller in real time, and is sent to the computer. The design of microcontroller module adds the flexibility of the robot system and reduces computation burdens of the computer.

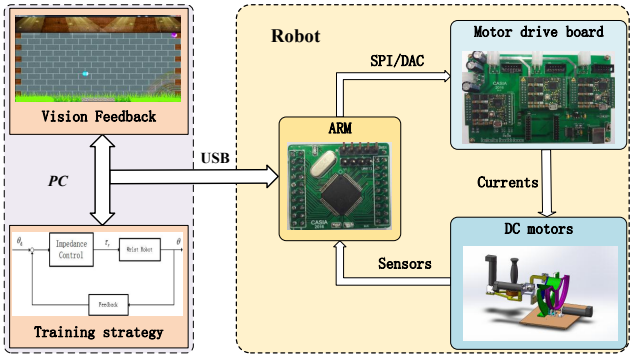

Fig. 2. Control architecture diagram

C. Safety

The mechanical hard-stop and mechanical emergency stop buttons are implemented to guarantee the safety of the subject. In addition, we adopt a current saturation mechanism in the software to limit the amount of torque of motors. Moreover, to reduce the risk of unexpected operations on the computer, a security strategy is applied in the ARM microcontroller: if the microcontroller does not receive the computer commands or receive invalid commands continuously, it will stop the motors or keep their current states.

D. Gravity Compensation

To decrease the influence of the self-gravity on the performance of the controller, we need to consider the gravity compensation for the controller design. All mechanical parts of the robot device are made of aluminum, and the mass of the mechanism can be neglected compared to the mass of the motors. Therefore, the implementation of gravity compensation is mainly focused on offsetting the gravity of the motors. The motor of P/S joint is fixed on the base and the other two motors do not impact the robot's F/E joint, we just need to consider what the gravity of the other two motors contribute to the robot's P/S and A/A joints, respectively.

The simplified kinematics of the mechanical structure is shown in Fig. 3, where the P/S and A/A robot joints are depicted. In the neutral position, Y_0, X_1 are coincident with the rotation axes of P/S and A/A joints, respectively. The frame $\{O_0\}$ is the basic coordinate and located at the crossing point of the P/S and A/A rotation axes. The rotation angle θ_1 and θ_2 correspond to the angles of the P/S and A/A joints. The frame $\{O_1\}$ rotates with angle θ_1 about axis Y_0, and the frame $\{O_2\}$ rotates with angle θ_2 about the axis X_1. P_{G1} and P_{G2} are the centers of mass (COM) of the motor of the A/A and F/E joints, respectively. The gravity compensation is defined as:

$$\tau_{G1}^{\theta_1} = \left[P_{G1}^{O_0} \times G_1^{O_0} \right]_{\{Y\}} \tag{1}$$

TABLE I
COMPARISON OF THE ROM AND MAXIMUM OUTPUT TORQUE OF THE WRIST ROBOT WITH THE REQUIREMENTS OF ADL

Wrist Joint	ADL		Robot	
	ROM(deg)	Torque(Nm)	ROM(deg)	Torque(Nm)
Pronation/Supination	150	0.06	170	3.05
Flexion/Extension	115	0.35	180	3.63
Adduction/Abduction	70	0.35	90	3.48

$$\tau_{G2}^{\theta_1} = \left[P_{G2}^{O_0} \times G_2^{O_0}\right]_{\{Y\}} \tag{2}$$

$$\tau_{G2}^{\theta_2} = \left[P_{G2}^{O_1} \times G_2^{O_1}\right]_{\{X\}} \tag{3}$$

where, the $\tau_{G1}^{\theta_1}$, $\tau_{G2}^{\theta_1}$ and $\tau_{G2}^{\theta_2}$ are the moment of gravity G_1 and G_2 about the axis Y_0 and the moment of gravity G_2 about the axis X_1, $P_{G1}^{O_1} = (x_1, y_1, z_1)^T$, $P_{G2}^{O_2} = (x_2, y_2, z_2)^T$ are the vectors P_{G1} and P_{G2} described in frame $\{O_1\}$ and frame $\{O_2\}$, respectively. $G_1^{O_0}$, $G_2^{O_0}$ and $G_2^{O_1}$ are the gravity forces described in the corresponding coordinate frames, and $\left[P_{G1}^{O_0} \times G_1^{O_0}\right]_{\{Y\}}$ is the Y-axis component of the cross product of $P_{G1}^{O_0}$ and $G_1^{O_0}$.

$$P_{G_1}^{O_0} = R_y(\theta_1) P_{G1}^{O_1} \tag{4}$$

$$P_{G_2}^{O_0} = R_y(\theta_1) R_x(\theta_2) P_{G2}^{O_2} \tag{5}$$

$$P_{G_2}^{O_1} = R_x(\theta_2) P_{G2}^{O_2} \tag{6}$$

$$G_2^{O_1} = R_x(-\theta_1) G_2^{O_0} \tag{7}$$

where $R_x(*)$ and $R_y(*)$ are the basic rotation matrices. Substituting (4)-(7) into (1)-(3), we can obtain:

$$\tau_{G1}^{\theta_1} = m_1 \mathrm{g} \left(x_1 \cos(\theta_1) + z_1 \sin(\theta_1)\right) \tag{8}$$

$$\tau_{G2}^{\theta_1} = m_2 \mathrm{g} \left[x_2 \cos(\theta_1) + \left(y_2 \sin(\theta_2) + z_2 \cos(\theta_2)\right) \sin(\theta_1)\right] \tag{9}$$

$$\tau_{G2}^{\theta_2} = -m_2 \mathrm{g} \cos(\theta_1) \left(y_2 \cos(\theta_1) - z_2 \sin(\theta_2)\right) \tag{10}$$

where m_1 and m_2 are the mass of the motors of the A/A and F/E joints.

III. CONTROLLER DESIGN AND EXPERIMENTS RESULTS

Robot-assist therapy is that robots replace therapists to assist patients to conduct rehabilitation exercises. Rehabilitation training has a strict requirement of the compliance and safety on the robot system. Impedance control proposed by Hogan [11] has been widely applied in human-robot interactions. Especially, impedance control is the primary control paradigm used in rehabilitation robot, because it can provide a compliant interaction between the subject and the robot. The inertia component of impedance control can be neglected due to the low acceleration of rehabilitation training motion. Thus, implementing impedance control on each robot joint, we obtain:

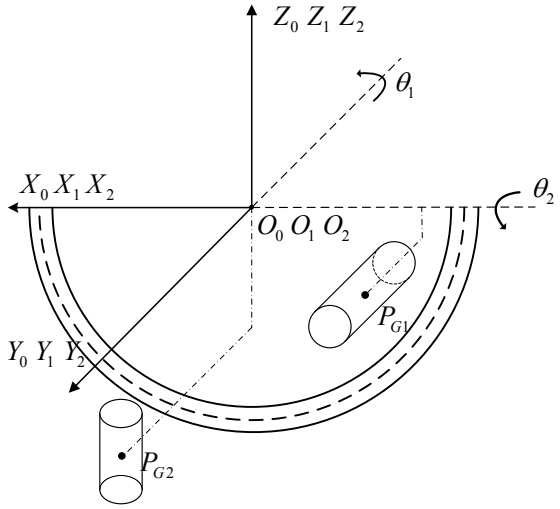

Fig. 3. Simplified kinematic of the mechanism

$$\tau_r = K(\theta_d - \theta) - B\dot{\theta} + G(\theta) \tag{11}$$

where θ_d, θ and $\dot{\theta}$ are the desired, actual angular position and angular speed of the joint, respectively. K and B are the stiffness and damping coefficient of the impedance control. $G(\theta)$ is the gravity compensation as described in the above section.

Since the reference trajectory is predefined, the classical impedance control might limit the voluntary participation of patients to some extent. If the stiffness is set lower, the robot may not keep the patient's motion in correct patterns. However, higher stiffness could lead to an unsafe or uncomfortable interaction as the patient deviates much from the desired trajectory. Moreover, it might lead patients to slack as patients relies much on the assistance provided by the robot. Inspired by the virtual tunnel proposed by Duschau-Wicke [12], we applied a "moving window" along with the reference trajectory, where the robot will not provide assistant forces when the patient moves within or ahead of the window. In addition, the predefined reference trajectory will be adjusted if patients move ahead of the window. The definition of "moving window" controller is:

$$\tau_a = \begin{cases} G(\theta) & \text{if } \theta \geq \theta_d - \frac{1}{2}w \\ K(\theta_d - \frac{1}{2}w - \theta) - B\dot{\theta} + G(\theta) & \text{if } \theta < \theta_d - \frac{1}{2}w \end{cases} \tag{12}$$

$$\theta_d(t) = \begin{cases} \hat{\theta}_d(t) + \Delta & \text{if } \theta \geq \theta_d + \frac{1}{2}w \\ \hat{\theta}_d(t) & \text{if } \theta < \theta_d + \frac{1}{2}w \end{cases} \tag{13}$$

where τ_a is the actual torque applied to the robot joint, $\hat{\theta}_d(t)$ and $\theta_d(t)$ are the predefined and actual reference trajectory, respectively. w is the width of the moving window and Δ is used to adjust the predefined reference trajectory as the patient moves ahead of the window. It should be noted that (12) and (13) correspond to the positive motion direction, and the criteria of equations need to be modified as the motion direction is negative.

To validate the feasibility and safety of the robot device, preliminary test experiments are implemented with a healthy volunteer. The above impedance controller and the "moving window" controller are tested on the robot's P/S joint, where K, B and w are set as 30 Nm/rad, 0.25 Nm/rad/s and 0.2 rad, and Δ is set equal to $\theta - (\theta_d + \frac{1}{2}w)$, while the other two joints are maintained in the neutral position. Meanwhile, the volunteer is allowed to apply voluntary forces to the robot, where the results are shown in Fig. 4. Compared with the impedance controller, "moving window" controller leads to a larger error between the actual joint position and the reference trajectory. However, it should be noted that for most of times the actual trajectory is ahead of the reference trajectory in the case of "moving window" controller. In other words, "moving window" controller can stimulate and permit more voluntary efforts of the participant instead of limiting the participant in a fixed trajectory.

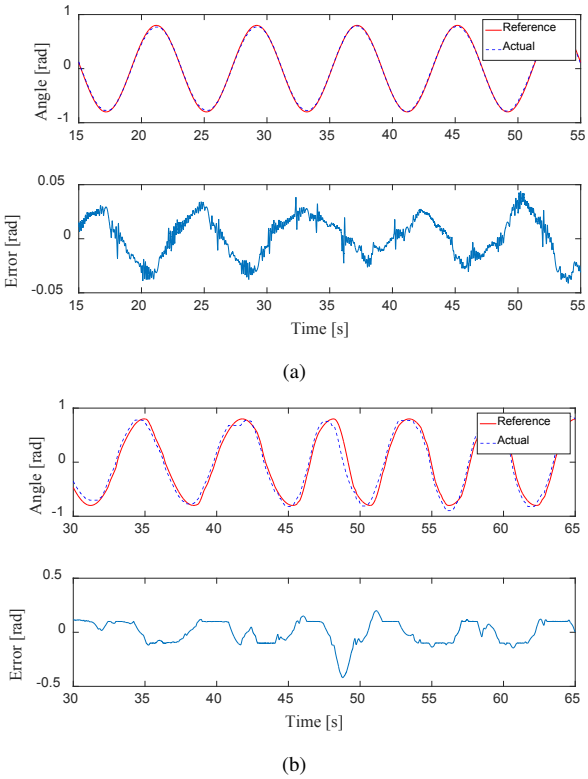

Fig. 4. Comparison between impedance control and "moving window" control. (a) impedance controller. (b) "moving window" controller.

IV. Conclusion

This paper presents the detailed design of a 3-DOF forearm-wrist rehabilitation robot system, including the mechanical structure design, control system design and gravity compensation analysis. The experiment results show that the proposed "moving window" controller has more potential than classical impedance controller in terms of stimulating the voluntary efforts of participants. In the future, the information of interactive forces and muscle electromyography (EMG) will be adopted to the robot system for increasing the adaptability of the rehabilitation robot.

References

[1] V. S. Huang and J. W. Krakauer, "Robotic neurorehabilitation: a computational motor learning perspective," *Journal of Neuroengineering and Rehabilitation*, vol. 6, no. 1, p. 1, 2009.

[2] D. Jack, R. Boian, A. S. Merians, M. Tremaine, G. C. Burdea, S. V. Adamovich, M. Recce, and H. Poizner, "Virtual reality-enhanced stroke rehabilitation," *IEEE Transactions on Neural Systems and Rehabilitation Engineering*, vol. 9, no. 3, pp. 308–318, 2001.

[3] H. I. Krebs, N. Hogan, M. L. Aisen, and B. T. Volpe, "Robot-aided neurorehabilitation," *IEEE Transactions on Rehabilitation Engineering*, vol. 6, no. 1, pp. 75–87, 1998.

[4] R. Sanchez, D. Reinkensmeyer, P. Shah, J. Liu, S. Rao, R. Smith, S. Cramer, T. Rahman, and J. Bobrow, "Monitoring functional arm movement for home-based therapy after stroke," in *Proceedings of Annual International Conference of the IEEE Engineering in Medicine and Biology Society (EMBC)*, 2004, pp. 4787–4790.

[5] P. S. Lum, C. G. Burgar, M. Van der Loos, P. C. Shor *et al.*, "Mime robotic device for upper-limb neurorehabilitation in subacute stroke subjects: A follow-up study," *Journal of Rehabilitation Research and Development*, vol. 43, no. 5, pp. 631 – 642, 2006.

[6] T. Nef, M. Mihelj, and R. Riener, "Armin: a robot for patient-cooperative arm therapy," *Medical & Biological Engineering & Computing*, vol. 45, no. 9, pp. 887–900, 2007.

[7] G. Kwakkel, B. J. Kollen, and H. I. Krebs, "Effects of robot-assisted therapy on upper limb recovery after stroke: a systematic review," *Neurorehabilitation and Neural Repair*, vol. 22, no. 2, pp. 111 – 121, 2007.

[8] J. Mehrholz, A. Hädrich, T. Platz, J. Kugler, and M. Pohl, "Electromechanical and robot-assisted arm training for improving generic activities of daily living, arm function, and arm muscle strength after stroke," *The Cochrane Library*, 2012.

[9] H. I. Krebs, B. T. Volpe, D. Williams, J. Celestino, S. K. Charles, D. Lynch, and N. Hogan, "Robot-aided neurorehabilitation: a robot for wrist rehabilitation," *IEEE Transactions on Neural Systems and Rehabilitation Engineering*, vol. 15, no. 3, pp. 327 – 335, 2007.

[10] A. Basteris, S. M. Nijenhuis, A. H. Stienen, J. H. Buurke, G. B. Prange, and F. Amirabdollahian, "Training modalities in robot-mediated upper limb rehabilitation in stroke: a framework for classification based on a systematic review," *Journal of Neuroengineering and Rehabilitation*, vol. 11, no. 1, pp. 1 – 15, 2014.

[11] N. Hogan, "Impedance control: An approach to manipulation: Part iiimplementation," *Journal of Dynamic Systems, Measurement, and Control*, vol. 107, no. 1, pp. 8–16, 1985.

[12] A. Duschau-Wicke, J. von Zitzewitz, A. Caprez, L. Lunenburger, and R. Riener, "Path control: a method for patient-cooperative robot-aided gait rehabilitation," *IEEE Transactions on Neural Systems and Rehabilitation Engineering*, vol. 18, no. 1, pp. 38–48, 2010.